DR CHENGYE CHE (Orcid ID : 0000-0001-9270-0693)

Article type : Original Article

Osteopontin contributes to effective neutrophils recruitment, IL-1β production, and apoptosis in *Aspergillus fumigatus* keratitis

Running title: Role of OPN in A. fumigatus keratitis

Guiqiu Zhao¹, Ming Hu², Cui Li¹, Jieun Lee³, Kelan Yuan¹, Guoqiang Zhu¹, Chengye Che^{1*}

1 Department of Ophthalmology, the Affiliated Hospital of Qingdao University, Qingdao, China; 2 Department of Basic Medical Sciences, Qingdao University, Qingdao, China; 3 Department of Ophthalmology, School of Medicine, Pusan National University, Yangsan, Korea

Correspondence: Chengye Che, Department of Ophthalmology, the Affiliated Hospital of Qingdao University, Qingdao 266003, China

E-mail: chechengye@126.com

This article has been accepted for publication and undergone full peer review but has not been through the copyediting, typesetting, pagination and proofreading process, which may lead to differences between this version and the Version of Record. Please cite this article as doi: 10.1111/imcb.12010

Keywords: Osteopontin; Fungal keratitis; *Aspergillus fumigatus*; Innate immunity; LOX-1; Interleukin 1 beta

Abstract

Fungal keratitis is a major cause of corneal ulcers, resulting in significant visual impairment and blindness. A phosphorylated glycoprotein secreted by immunocompetent cells, osteopontin (OPN) mediates cluster formation of the host fungal receptors and enhances the phagocytosis and clearance of pathogenic fungi. However, whether OPN production and function occurs in fungal keratitis is unknown. OPN expression in Aspergillus fumigatus keratitis patient corneas was assessed by quantitative polymerase chain reaction (qRT-PCR) and immunofluorescence. Human neutrophils, THP-1 macrophages, and corneal epithelial cells (HCECs) stimulated with A. fumigatus were utilized for in vitro experiments. Mouse models of A. fumigatus keratitis were developed by intra-stromal injection for in vivo experiments. Using siRNAs, neutralizing antibodies, recombinant proteins and inhibitors, the production and role of OPN in A. fumigatus infection was assessed by clinical evaluation, qRT-PCR, immunofluorescence, western blotting and bioluminescence image acquisition. We observed increased corneal OPN expression in *A. fumigatus* keratitis patients and mouse models compared to controls. OPN production in response to A. fumigatus infection was dependent on LOX-1 and Erk1/2. Compared to controls, OPN knockdown impaired pro-inflammatory cytokine IL-1 β production, which was dependent upon 4E-BP1. OPN knockdown decreased MPO levels and resulted in decreased neutrophil recruitment, higher

fungal load, and increased apoptosis in mouse *A. fumigatus* keratitis. Our results indicate that OPN is a critical component of the antifungal immune response and is essential for effective neutrophil recruitment, inflammatory cytokine production and apoptosis in *A. fumigatus* keratitis.

INTRODUCTION

The incidence of fungal keratitis is increasing worldwide, and the aetiological agents most commonly responsible are filamentous *Aspergillus* species (*A. fumigatus, A. flavus*) and *Fusarium* (*F. solani, F. oxysporum*)¹. The impact of fungal keratitis on visual health accounts for up to 60% of corneal ulcers attributable to fungal infection in developing countries, including China, India and Mexico¹⁻³. Even in developed countries, such as the United States, fungal keratitis accounts for up to 35% of all corneal ulcers, resulting in severe visual impairment and blindness^{1, 4}. Although new therapies are being used in clinical application, fungal keratitis remains a challenge to ophthalmologists because of delayed diagnosis and a lack of effective drugs and treatment methods⁵.

Innate immunity is the first line of defence against pathogenic fungi during fungal keratitis. Pattern recognition receptors (PRRs) and C-type lectin receptors (CLRs), for example, dendritic cell-associated c-type lectin-1 (dectin-1) and lectin-type oxidized LDL receptor 1 (LOX-1), play important roles in antifungal immunity ^{1, 6}. In host immune defence against *Pneumocystis*, cluster formation of antifungal receptors, including dectin-1, Toll-like receptor 2 (TLR2) and mannose receptor (MR), is dependent on osteopontin (OPN), an

adaptor molecule in TLR2 and Dectin-1 signalling pathways mediates ERK activation and cytokine production and enhances the phagocytosis and clearance of pathogenic fungi⁷.

OPN, encoded by the secreted phosphoprotein 1 (SPP1) gene, is expressed in a range of immune cells, including macrophages, neutrophils, dendritic cells, and T and B cells, where it acts as an immune modulator in a variety of ways ⁸⁻¹¹. First, OPN has chemotactic properties that promote cell recruitment to inflammatory sites ^{12, 13}. It also functions as an adhesion protein involved in cell attachment and wound healing ^{14, 15}. In addition, OPN mediates cell activation and cytokine production, as well as promoting cell survival by regulating apoptosis ¹⁶⁻¹⁹. Furthermore, OPN is involved in granuloma formation and in modulating the severity of *Paracoccidioides brasiliensis* infection ²⁰. *In vivo*, OPN-deficient mice show increased susceptibility to low load, but not high load, fungal infection ²¹. However, the production and role of OPN in fungal keratitis has not been reported.

This study demonstrates that OPN is increased in the cornea of *A. fumigatus* keratitis patients and a variety of additional cell types that are pivotal anti-fungal infection cells found in the cornea, including corneal epithelial cells, macrophages and neutrophils. Upon *A. fumigatus* infection, OPN production occurs in a LOX-1- and Erk1/2-dependent fashion. OPN knockdown impaired pro-inflammatory cytokine IL-1β production induced by *A. fumigatus* infection, which was dependent on the eukaryotic translation initiation factor 4E-binding protein 1 (4E-BP1). A relatively mild inflammatory response and decreased neutrophil recruitment were observed in response to knockdown of OPN, which might be

related to increased apoptosis in *A. fumigatus*-infected corneas. These data suggest that OPN is a critical component of the antifungal immune response in *A. fumigatus* keratitis.

RESULTS

OPN levels are increased in human *A. fumigatus* keratitis and *A. fumigatus*-stimulated neutrophils, THP-1 macrophages and HCECs

OPN mRNA (Figure 1a) and protein levels (Figure 1b) were significantly higher in the corneas of *A. fumigatus* patients compared to healthy controls. OPN mRNA levels in neutrophils (Figure 1c), THP-1 macrophages (Figure 1e) and HCECs (Figure 1g) were higher after stimulation with *A. fumigatus* for 4 and 16 hours compared to controls. In addition, the OPN protein levels measured by western blotting were elevated in stimulated neutrophils (Figure 1d), macrophages (Figure 1f) and HCECs (Figure 1h) at 16-hours post-*A. fumigatus* infection compared to controls.

OPN levels increase in response to A. fumigatus keratitis in mice

Figure 2a shows that at 1 day post-infection, C57BL/6 mice developed significant corneal opacity, which persisted up to 14 days post-infection. With increased neovascularization, corneal inflammation gradually improved. Compared with controls, OPN mRNA levels in mouse corneas were significantly higher after 12-hour *A. fumigatus* infection, peaking at 3 days and persisting up to 10 days post-infection (Figure 2b). OPN protein levels were

elevated in infected mouse corneas at 12 hours compared with controls, which persisted up to 7 days post-infection (Figure 2c). Increased OPN was also confirmed by immunostaining. The results showed that OPN protein expression markedly increased in infected mouse corneas 1 day post-infection compared to controls (Figure 2d).

Aspergillus fumigatus-induced OPN production is dependent on LOX-1 and Erk1/2 and independent of Dectin-1 and JNK

Photographs taken by a slit lamp at 1 day post-infection illustrate the disease response in scrambled control versus siRNA_{LOX-1}-treated mice (Figure 3a). LOX-1 silencing was assessed by clinical score (Figure 3b), fungal survival (Figure 3c) and protein expression (Figure 3e), which confirmed efficient gene knockdown. OPN mRNA (Figure 3d) and protein (Figure 3e) levels in mouse corneas with siRNA_{LOX-1} treatment were significantly lower after *A*. *fumigatus* infection. However, no significant differences were observed in corneal OPN expression of mice treated with siRNA_{Dectin-1}(Supplementary figure 1a-e).

The role of LOX-1 and Dectin-1 in OPN production upon *A. fumigatus* infection were confirmed using HCEC *in vitro*. After LOX-1 neutralization, expression of IL-1β protein was significantly down-regulated (Figure 3g), confirming its neutralization function. LOX-1 neutralization decreased the mRNA (Figure 3f) and protein (Figure 3g) expression of OPN. However, no significant differences in OPN expression were observed in mice treated with Dectin-1 neutralization (Supplementary figure 1f, g).

Erk1/2 and JNK functions in OPN production in response to *A. fumigatus* infection were confirmed in mouse models and HCEC experiments. The efficacy of the Erk1/2 inhibitor SCH772984 was confirmed by measuringErk1/2 protein phosphorylation levels *in vivo* (Figure 3i) and *in vitro* (Figure 3k). The Erk1/2 inhibitor decreased mRNA and protein expression of OPN *in vivo* (Figure 3h and i) and *in vitro* (Figure 3j and k). However, no significant differences in OPN expression were observed in mice treated with a JNK inhibitor (Supplementary figure 1h-k).

Disease response after siRNA_{OPN} treatment

Photographs taken by slit lamp at 1 day (Figure 4a) and 2 days (Figure 4f) post-infection illustrate the disease response in scrambled control versus siRNA_{OPN}-treated mice. The palliative disease response is represented by a clinical score, which was significantly higher at 1 day (Figure 4b) and 2 days (Figure 4g) in scrambled siRNA-treated controls compared to siRNA_{OPN}-treated mice. Compared with scrambled siRNA-treated controls, siRNA_{OPN}-treated mice exhibited a higher CFU at 1 day (Figure 4c) and 2 days (Figure 4h). OPN silencing was assessed by mRNA and protein detection at 1 day (Figure 4d, e) and 2 days (Figure 4i, j), which confirmed efficient gene knockdown.

4E-BP1

siRNA_{OPN} treatment reduced neutrophil infiltration and MPO activity in *A. fumigatus* keratitis mice

NIMP-R14 was stained in the corneas of siRNA_{OPN} and scrambled siRNA-treated mice at 1 day post-infection (Figure 5a). Positive staining (green) in the corneas of siRNA_{OPN} mice indicated the decreased presence of neutrophils compared to scrambled siRNA-treated control mice. Average bioluminescence, measured by an inflammation probe dropped into the surface of mouse cornea, revealed that corneas of siRNA_{OPN}-treated mice exhibited a significant decrease in MPO levels at 1 day post-infection compared to scrambled controls (Figure 5b, c). Traditional MPO detection methods using a colorimetric activity assay showed a similar result (Figure 5d).

OPN-mediated IL-1β secretion in response to *A. fumigatus* infection is dependent on 4E-BP1

Compared to controls, IL-1 β protein levels in *A. fumigatus*-infected mouse corneas were significantly higher after 12 hours, persisting up to 10 days post-infection (Figure 6a). IL-1 β mRNA (Figure 6b) and protein (Figure 6c) levels in mouse corneas exposed to siRNA_{OPN} treatment were significantly lower after *A. fumigatus* infection. Decreased IL-1 β mRNA and protein levels were rescued by the addition of rmOPN (Figure 6d and e). The role of OPN in IL-1 β production upon *A. fumigatus* infection was also confirmed in HCEC experiments. OPN neutralization decreased the expression of IL-1 β mRNA (Figure 6f) and protein (Figure 6g), which was rescued by the addition of rhOPN (Figure 6h, i).

Compared to scrambled siRNA-treated controls, phosphorylation levels of 4E-BP1 in mouse corneas in response to siRNA_{OPN} treatment significantly decreased after *A. fumigatus* infection (Figure 6c). Decreased IL-1 β mRNA and protein levels induced by siRNA_{OPN} treatment were rescued by the addition of a 4E-BP1/eIF4E interaction inhibitor, 4E1RCat (Figure 6j and k). *In vitro* experiments showed a similar result (Figure 6l, m).

siRNA_{OPN} treatment increased levels of apoptosis in A. fumigatus keratitis mice

Compared to scrambled siRNA-treated controls, Bcl-2 mRNA levels (Figure 7a) in siRNA_{OPN}-treated mouse corneas were significantly decreased. BAX (Figure 7b) and caspase-3 (Figure 7c) increased after infection with *A. fumigatus*. The correlative results obtained from western blotting indicated that phosphorylated Akt and Bcl-2 levels significantly decreased, while BAX, cleaved-caspase-3 and cleaved-caspase-9 were significantly increased with siRNA_{OPN} treatment (Figure 7d). However, cleaved-caspase-8 was not affected by siRNA_{OPN} treatment.

DISCUSSION

This study demonstrates that OPN contributes to effective neutrophil recruitment, inflammatory cytokine production and apoptosis in *A. fumigatus* keratitis mice. These findings indicate that OPN may be a critical component of the antifungal immune response in the cornea. Although the role of OPN in mediating fungal keratitis is still not well

understood, several studies indicate its role in antifungal immunity. For example, Inoue *et al.*¹⁹ found that OPN is essential in mediating the cluster formation of fungal receptors that detect *Pneumocystis* and plays a role as an adaptor molecule in the TLR2 and Dectin-1 signalling pathways. Nishikaku *et al.*^{20, 22} found that OPN is involved in granuloma formation and in the severity of *Paracoccidioides brasiliensis* infection. Sato I *et al.*²¹ found that OPN-deficient mice exhibited increased susceptibility to low fungal load. Taken together, these observations are consistent with our results that OPN plays a critical role in host antifungal immunity.

In addition, we observed increased expression of OPN in human neutrophils, macrophages and corneal epithelial cells in response to *A. fumigatus* infection. Although the cornea is considered an immune privileged region, it has been well established that macrophage cells reside in the corneal stroma and epithelium ²³. Furthermore, neutrophils were shown to be the first cells recruited to the cornea to fight fungal infection ²⁴. Human corneal epithelial cells are involved in antifungal immunity by way of releasing antimicrobial peptides, inflammatory cytokines and chemokines ^{25, 26}. The role of OPN in human neutrophils and macrophages in antifungal immunity has been described, but OPN has not previously been examined corneal epithelial cells solely involved in corneal wound healing ²⁷. Importantly, our study demonstrates that human corneal epithelial cells participate in antifungal immunity by producing OPN.

Production of OPN upon *A. fumigatus* infection is dependent on LOX-1 but not Dectin-1 expression. This observation is consistent with reports showing that OPN expression increased in wild-type mouse models of ischaemia-reperfusion but to a much smaller extent in LOX-1 KO mice ^{28, 29}. This finding indicates that the LOX-1 membrane receptor is responsible for initiating the expression of intracellular OPN in order to cope with corresponding signals. These findings also indicate that Erk1/2, not JNK, contributes to the amplification of OPN production upon *A. fumigatus* infection.

Furthermore, compared to the normal course of disease in C57BL/6 mice, knockdown of OPN resulted in a reduced clinical score and impaired fungal clearance. Decreased corneal neutrophil recruitment and MPO activity may be responsible for this. As the peroxidase enzyme converts chloride and hydrogen peroxide into hypochlorous acid during the respiratory burst phase, MPO measured by bioluminescence imaging and colorimetric activity assay is used by the neutrophil to kill fungi and other pathogens. Singh R *et al.*⁹ found that reduced neutrophil accumulation in the absence of OPN was accompanied by an increase in bacterial load. Barreno *et al.*³⁰ also found that following O₃exposure, bronchoalveolar lavage fluid neutrophil levels were significantly reduced in OPN-deficient mice compared with wild-type mice. These findings indicate that OPN plays a critical role in the recruitment of neutrophils during the inflammatory response.

Similar to cellular infiltration, OPN knockdown corneas exhibited impaired pro-inflammatory cytokine IL-1 β production compared with control corneas. As a critical mediator of the host response to microbial infections, IL-1 β is involved in a variety of cellular activities, including

cell proliferation, apoptosis and differentiation. These results are consistent with reports on *Pseudomonas aeruginosa*-induced bacteraemia in which OPN-KO mice exhibited reduced secretion of pro-inflammatory cytokines, such as interferon- γ , IL-1 β , IL-12 and tumour necrosis factor- α ³¹. OPN knockdown also decreased 4E-BP1 phosphorylation, and IL-1 β decreased by OPN knockdown was rescued by treatment with a 4E-BP1/eIF4E interaction inhibitor. This result is consistent with reports on lung tumourigenesis in which triple mutant OPN was observed to decrease NF- κ B activity and 4E-BP1 phosphorylation³². Previous studies have also shown phosphorylation of mammalian target of rapamycin (mTOR)/4E-BP1 pathways increased IL-1 β expression^{33, 34}. 4E-BP1 is one member of a large family of translation repressor proteins that directly interact with the eukaryotic translation initiation factor 4E (eIF4E). The interaction of 4E-BP1 with eIF4E inhibits complex assembly and represses translation. 4E-BP1 is phosphorylated in response to various signals, including UV irradiation and insulin signalling, resulting in its dissociation from eIF4E and activation of cap-dependent mRNA translation.

Infection and apoptosis as a combined inflammatory trigger are best suited for clearing infecting pathogens and repairing damage to host tissue during infection ³⁵. In this study, OPN knockdown increased mitochondrial-dependent apoptosis in mice with *A. fumigatus* keratitis. Inflammatory immune responses induce necrotic cell death of immunocytes and release damage-associated molecular patterns (DAMPs) to amplify the inflammation. However, apoptosis during infection can shape a suppressive, autoreactive, or protective immune response ³⁶. OPN seems to play an important physiological role in the efficient development of Th1 immune responses and cell survival by inhibiting apoptosis ³⁷⁻³⁹. These

findings indicate that OPN knockdown may reduce inflammation by modulating neutrophils recruitment, decreasing pro-inflammatory cytokines and increasing apoptosis.

In conclusion, our results demonstrate the essential pro-inflammatory role of OPN in *A. fumigatus* keratitis. We support these findings using a range of experimental models from patient corneas, *A. fumigatus* keratitis mice models and cell line experiments.

METHODS

Clinical specimens

Six healthy and six *A. fumigatus* keratitis corneas identified by a combination of morphology and fungal culture were used in this study. The ethics committee of the Affiliated Hospital of Qingdao University approved the corneas for use. The use of corneas has been described in previous publications from our laboratory ⁶. The research adhered to the tenets of the Declaration of Helsinki. The research aims and methodologies were thoroughly explained to patients, and informed consent was obtained to collect the samples. Patients with acute or chronic systemic illness or with any form of immunosuppression or topical steroid therapy were excluded from this study.

Preparing Aspergillus fumigatus

Aspergillus fumigatus strain 3.0772 was purchased from The China General Microbiological Culture Collection Center (Beijing, China). The strain was cultured for 3–4 days on a This article is protected by copyright. All rights reserved.

Sabouraud agar. Suspensions of fresh conidia scraped from the surface of the medium were quantified with a haemocytometer and adjusted to a final concentration of 5×10^4 conidia μ L⁻¹ in PBS.

In vitro experiments

Human neutrophil experiments were obtained from the peripheral blood of healthy volunteers and was approved by the ethics committee of the Affiliated Hospital of Qingdao University. Neutrophils were isolated by Ficoll Paque Plus (TBD, Tianjing, China) and suspended in a RPMI-1640 media (HyClone, Logan, UT, USA) at a density of 1×10⁶mL⁻¹. Giemsa staining showed >95% neutrophils.

THP-1 macrophages purchased from the China Center for Type Culture Collection (Wuhan, China) were differentiated with 100 nM of Phorbol 12-Myristate 13-Acetate (PMA) (Sigma, St. Louis, MO, USA) for 48hours and allowed to recover for 24 hours prior to infection. Macrophages were cultured in RPMI-1640 medium at a density of 1×10⁶ mL⁻¹.

Human corneal epithelial cells (HCECs) were provided by the Ocular Surface Laboratory at the Zhongshan Ophthalmic Center. Cells were cultured to 80% confluence in serum-free DMEM (HyClone, Logan, UT, USA) for 24 hours.

To study OPN expression, human neutrophils, THP-1 macrophages and HCECs were treated with *A. fumigatus* conidia in 12-well and 6-well plates at a multiplicity of infection (MOI) of 1 for 0, 1 and 4hours (qRT-PCR) and 0, 1/4, 1/2, 1, 4 and 16 hours (western blotting).

To study *A. fumigatus*-induced OPN expression and the role of OPN in antifungal immunity, HCECs were treated with neutralizing antibodies or inhibitors 2 hours before treatment with conidia. Neutralizing antibodies included a goat LOX-1 neutralizing antibody (R&D, Minneapolis, MN, USA) at a final concentration of 10 μ g mL⁻¹⁴⁰, a goat Dectin-1 neutralizing antibody (R&D) at a final concentration of 30 μ g mL⁻¹, a goat OPN neutralizing antibody (R&D) at a final concentration of 10 μ g mL⁻¹, a goat OPN neutralizing antibody (R&D) at a final concentration of 10 μ g mL⁻¹) ⁴¹, and a control goat IgG (R&D). Inhibitors included the JNK inhibitor SP600125 (SelleckChem, Houston, TX, USA) (40 μ M) ⁴², the Erk1/2 inhibitor SCH772984 (SelleckChem) (10 μ M) ⁴³ and the 4E-BP1/eIF4E interaction inhibitor 4E1RCat (SelleckChem) (50 μ M) ⁴⁴.

HCECs were treated with human osteopontin recombinant protein (rhOPN; R&D Systems) at a final concentration of 180 ng mL⁻¹) ⁴⁵ or 4E1RC at 1 hour after treatment with the OPN neutralizing antibody. After pretreatment, HCECs were treated with *A. fumigatus* conidia at an MOI of 1 for 0 and 16 hours in 12-well plates for qRT-PCR and 0 and 16 hours in 6-well plates for western blotting.

In vivo experiments

Eight-week-old C57BL/6 female mice were purchased from the Changzhou Cavens Laboratory (Jiangsu, China). Mice were treated in accordance with the *Statement for the Use* of Animals in Ophthalmic and Vision Research by the Association for Research in Vision and Ophthalmology (ARVO). Mice were anaesthetized with 8% chloral hydrate. *A. fumigatus* conidia $(0.5 \times 10^5 \mu L^{-1})$ were released into their corneal stroma, and mice were examined daily

by a slit lamp microscope for corneal opacification and ulceration. Ocular disease was graded using clinical scores ranging from 0 to 12 according to the scoring system by Wu *et* al. ⁴⁶.

To study the expression and role of OPN in A. fumigatus keratitis, two methods were used for inhibition: (1) siRNA treatment and (2) pharmacological inhibitors. SiRNA treatment was used for Dectin-1 (Santa Cruz, Santa Cruz, CA, USA), LOX-1 (Santa Cruz) and OPN (Santa Cruz) inhibition. Inhibitor treatments were used for JNK (SP600125; SelleckChem), Erk1/2 (SCH772984; SelleckChem) and 4E-BP1/eIF4E interaction (4E1RCat; SelleckChem) inhibition. For siRNA treatments, the eye randomly selected from mice received a subconjunctival injection (5 µL) containing 8 µM of siRNA or a non-targeting scrambled sequence (negative control) (Santa Cruz) 1 day and 2 hours before *A. fumigatus* infection ⁴⁷. For inhibitor treatments, the eye randomly selected from the mice received a subconjunctival injection (5 μ L) containing 40 μ M of SP600125, 10 μ M of SCH772984, or a DMSO control 1 day and 2 hours before infection ⁴⁸. To assess the function of OPN and 4E-BP1 in IL-1β secretion upon A. fumigatus infection, the randomly selected eye from the mouse received a subconjunctival injection (5 µL) containing 8 µM of OPN siRNA 1 day and 2 hours before infection, and a subconjunctival injection (5 μ L) containing 100 μ g mL⁻¹ of mice osteopontin recombinant protein (rmOPN; R&D) or 50 µM 4E1RC 1 hour before infection.

Quantification of Aspergillus colony forming units (CFUs)

To assess fungal viability, whole eyes were homogenized under sterile conditions in 1 mL of PBS using a Mixer Scientz-48 (Scientz, Ningbo, China) at 33 Hz for 4 minutes. Subsequently,

serial log dilutions were performed and plated onto Sabouraud dextrose agar plates (BDMS, Cockeysville, MD, USA). Following incubation for 24hours at 37°C, the number of CFUs was determined by direct counting.

Myeloperoxidase (MPO) assay

Corneas were cut at one day p.i. and homogenized in 1.0 mL of 50 mM phosphate buffer (pH 6.0) with 0.5% hexadecyltrimethyl-ammonium. Samples were freeze-thawed and centrifuged, and 100 μ L of supernatant was added to 2.9 mL phosphate buffer with O-Dianisidine dihydrochloride (0.167 mg mL⁻¹) and 0.0005% hydrogen peroxide. The absorbency (460 nm) was measured at 30-second intervals for 5 minutes. The slope of the line was determined in relation to the assay units of MPO/cornea.

RNA isolation and qRT-PCR

The mRNA levels of OPN and IL-1 β in human neutrophils, THP-1macrophages, HCECs and mouse corneas were detected after infection with *A. fumigatus*. The PCR protocol has been described in previous publications ⁶. The primer pair sequences are listed in Supplementary table 1.

For tissue immunofluorescence, human corneas and mouse eyes (n = 6/group/time) were embedded in an OCT compound (Tissue-Tek; Miles, Elkhart, IN, USA) and frozen in liquid nitrogen. The immunofluorescence protocol has been described in previous publications ⁶. Primary antibodies included 10 µg mL⁻¹ rabbit anti-human OPN antibody (ProteinTech, Chicago, IL, USA), a rabbit anti-mouse OPN antibody (ProteinTech) and a rat anti-mouse NIMP-R14 antibody (Santa Cruz). FITC-conjugated goat anti-rabbit antibody (1:200; Bioss, Beijing, China), Alexa Fluor 555-conjugated goat anti-rabbit antibody (1:1000; CST, Danvers, MA, USA,) and Alexa Fluor 488-conjugated goat anti-rat antibody (1:1000; CST) were secondary antibodies.

Western blotting

The western blotting protocol for corneas and cells has been described in previous publications ⁶. The primary antibodies are listed in Supplementary Table2. Blots were stained using the following HRP-tagged secondary antibodies purchased from CST.

Bioluminescence imaging and image acquisition and analysis

Bioluminescence images were captured and analysed by the *In Vivo* Imaging System (IVIS) spectrum (Perkin Elmer, Santa Clara, CA, USA). Imaging was performed one day after *A. fumigatus* conidia infection. Fifteen minutes before imaging, mice received an

intraperitoneal injection of 8% chloral hydrate. The luminescent reagent (MPO xenoLightrediJect inflammation probe; Perkin Elmer) was dropped onto the surface of the mouse cornea 7 minutes before imaging. Mice were positioned on the IVIS warming stage in the infected eye lateral decubitus position with the ocular surface directly facing the camera sensor. *In vivo* imaging parameters were determined using standard optimization protocols ^{49, 50}. Mice were imaged using a field of view 'C' with medium binning for 1 minute. Average bioluminescence at baseline and peak inflammation was compared by paired Student's *t*-test using Prism-5 software. Before *t*-test analysis, the normality present in the differences of paired data was tested by Shapiro-Wilk analysis with failure to reject the null hypothesis.

Statistical analysis

An unpaired two-tailed Student's *t*-test was used to determine the statistical significance of the qRT-PCR, western blotting, clinical score and CFU assays. Data were considered significant at $P \le 0.05$. All experiments were repeated once to ensure reproducibility, and data from a representative experiment are shown as the mean ± SD.

CONFLICT OF INTEREST

The authors declare no conflict of interest.

ACKNOWLEDGMENTS

This work was supported by National Natural Science Foundation of China 81300730 and by Independent Innovation Plan of Qingdao 16-5-1-65-jch.

References

- 1 Leal SM Jr, Cowden S, Hsia YC, *et al*. Distinct roles for Dectin-1 and TLR4 in the pathogenesis of *Aspergillus fumigatus* keratitis. *PLoS Pathog* 2010; **6**: e1000976.
- 2 Karthikeyan RS, Leal SM Jr, Prajna NV, *et al*. Expression of innate and adaptive immune mediators in human corneal tissue infected with *Aspergillus* or *fusarium*. *J Infect Dis* 2011; 204: 942-950.
- 3 Guo H, Gao J, Wu X. Toll-like receptor 2 siRNA suppresses corneal inflammation and attenuates *Aspergillus fumigatus* keratitis in rats. *Immunol Cell Biol* 2012; **90**: 352-357.
- 4 Thomas PA. Current perspectives on ophthalmic mycoses. *Clin Microbiol Rev* 2003; **16**: 730-797.
- 5 Wu H, Ong ZY, Liu S, *et al*. Synthetic β-sheet forming peptide amphiphiles for treatment of fungal keratitis. *Biomaterials* 2015; **43**: 44-49.
- 6 Li C, Zhao G, Che C, *et al*. The role of LOX-1 in innate immunity to *Aspergillus fumigatus* in corneal epithelial cells. *Invest Ophthalmol Vis Sci* 2015; **56**: 3593-3603.

7 Inoue M, Moriwaki Y, Arikawa T, *et al*. Cutting edge: critical role of intracellular osteopontin in antifungal innate immune responses. *J Immunol* 2011; **186**: 19-23.

- 8 Guo H, Mi Z, Bowles DE, *et al.* Osteopontin and protein kinase C regulate PDLIM2 activation and STAT1 ubiquitination in LPS-treated murine macrophages. *J Biol Chem* 2017; **292**: 1142.
- 9 Singh R, Hui T, Matsui A, *et al*. Modulation of infection-mediated migration of neutrophils and CXCR2 trafficking by osteopontin. *Immunology* 2017; **150**: 74-86.
- 10 Shao Z, Morser J, Leung LL. Thrombin cleavage of osteopontin disrupts a pro-chemotactic sequence for dendritic cells, which is compensated by the release of its pro-chemotactic C-terminal fragment. *J Biol Chem* 2014; **289**: 27146-27158.
- 11 Tahir S, Fukushima Y, Sakamoto K, *et al*. A CD153+CD4+ T follicular cell population with cell-senescence features plays a crucial role in lupus pathogenesis via osteopontin production. *J Immunol* 2015; **194**: 5725-5735.
- 12 Nishimichi N, Hayashita-Kinoh H, Chen C, *et al*. Osteopontin undergoes polymerization in vivo and gains chemotactic activity for neutrophils mediated by integrin alpha9beta1. *J Biol Chem* 2011; **286**: 11170-11178.

13 Many GM, Yokosaki Y, Uaesoontrachoon K, *et al*. OPN-a induces muscle inflammation by increasing recruitment and activation of pro-inflammatory macrophages. *Exp Physiol* 2016; **101**: 1285-1300.

14 Frank JW, Seo H, Burghardt RC, *et al*. ITGAV (alpha v integrins) bind SPP1 (osteopontin) to support trophoblast cell adhesion. *Reproduction* 2017; **153**: 695-706.

15 Miyazaki K, Okada Y, Yamanaka O, *et al*. Corneal wound healing in an osteopontin-deficient mouse. *Invest Ophthalmol Vis Sci* 2008; **49**: 1367-1375.

16 Tsai CH, Liu SC, Wang YH, et al. Osteopontin inhibition of miR-129-3p enhances IL-17 expression and monocyte migration in rheumatoid arthritis. *Biochim Biophys Acta* 2017; 1861: 15-22.

- 17 Zhao K, Zhang M, Zhang L, *et al.* Intracellular osteopontin stabilizes TRAF3 to positively regulate innate antiviral response. *Sci Rep* 2016; **6**:23771.
- 18 Kawakami K, Minami N, Matsuura M, *et al.* Osteopontin attenuates acute gastrointestinal graft-versus-host disease by preventing apoptosis of intestinal epithelial cells. *Biochem Biophys Res Commun* 2017; **485**: 468-475.
- 19 Huang RH, Quan YJ, Chen JH, *et al.* Osteopontin promotes cell migration and invasion, and inhibits apoptosis and autophagy in colorectal cancer by activating the p38 MAPK signaling pathway. *Cell Physiol Biochem* 2017; **41**: 1851-1864.
- 20 Nishikaku AS, Scavone R, Molina RF, et al. Osteopontin involvement in granuloma formation and in the severity of *Paracoccidioides brasiliensis* infection. *Med Mycol* 2009;
 47:495–507.
- 21 Sato I, Yamamoto N, Rittling SR, *et al*. Osteopontin is dispensable for protection against high load systemic fungal infection. *Int Immunopharmacol* 2008; **8**:1441–1448.

22 Nishikaku AS, Molina RF, Ribeiro LC, *et al*. Nitric oxide participation in granulomatous response induced by *Paracoccidioides brasiliensis* infection in mice. *Med Microbiol Immunol* 2009; **198**: 123-135.

- 23 Brissette-Storkus CS, Reynolds SM, Lepisto AJ, *et al*. Identification of a novel macrophage population in the normal mouse corneal stroma. *Invest Ophthalmol Vis Sci* 2002;
 43:2264–2271.
- 24 Taylor PR, Roy S, Leal SM Jr, *et al*. Activation of neutrophils by autocrine IL-17A-IL-17RC interactions during fungal infection is regulated by IL-6, IL-23, RORγt and dectin-2. *Nat Immunol* 2014; **15**: 143-151.
- 25 Gao N, Yu FS. Chitinase 3-Like 1 promotes *Candida albicans* killing and preserves corneal structure and function by controlling host antifungal responses. *Infect Immun* 2015; 83: 4154-4164.
- 26 Hua X, Yuan X, Li Z, *et al*. A novel innate response of human corneal epithelium to heat-killed *Candida albicans* by producing peptidoglycan recognition proteins. *PLoS One* 2015; **10**: e0128039.
- 27 Yamanaka O, Sumioka T, Saika S. The role of extracellular matrix in corneal wound healing. *Cornea* 2013; **32**:S43-45.
- 28 Hu C, Dandapat A, Chen J, et al. LOX-1 deletion alters signals of myocardial remodeling immediately after ischemia-reperfusion. *Cardiovasc Res* 2007; **76**: 292-302.

29 Hu C, Dandapat A, Sun L, *et al.* LOX-1 deletion decreases collagen accumulation in atherosclerotic plaque in low-density lipoprotein receptor knockout mice fed a high-cholesterol diet. *Cardiovasc Res* 2008; **79**: 287-293.

30 Barreno RX, Richards JB, Schneider DJ, *et al*. Endogenous osteopontin promotes ozone-induced neutrophil recruitment to the lungs and airway hyperresponsiveness to methacholine. *Am J Physiol Lung Cell Mol Physiol* 2013; **305**: L118-129.

31 Piao Z, Yuan H. Osteopontin exacerbates *Pseudomonas aeruginosa*-induced bacteremia in mice. *Cell Immunol* 2017; **318**: 23-28.

- 32 Minai-Tehrani A, Chang SH, Kwon JT, *et al*. Aerosol delivery of lentivirus-mediated O-glycosylation mutant osteopontin suppresses lung tumorigenesis in K-ras (LA1) mice. *Cell Oncol (Dordr)* 2013; **36**: 15-26.
- 33 Zhou W, Guo S, Gonzalez-Perez RR. Leptin pro-angiogenic signature in breast cancer is linked to IL-1 signalling. *Br J Cancer* 2011; **104**: 128-137.
- Pan H, Xu LH, Ouyang DY, et al. The second-generation mTOR kinase inhibitor INK128 exhibits anti-inflammatory activity in lipopolysaccharide-activated RAW 264.7 cells.
 Inflammation 2014; 37: 756-765.
- 35 Torchinsky MB, Garaude J, Blander JM. Infection and apoptosis as a combined inflammatory trigger. *Curr Opin Immunol* 2010; **22**: 55-62.
- 36 Campisi L, Cummings RJ, Blander JM. Death-defining immune responses after apoptosis. *Am J Transplant* 2014; **14**: 1488-1498.

37 Kawakami K, Minami N, Matsuura M, *et al.* Osteopontin attenuates acute gastrointestinal graft-versus-host disease by preventing apoptosis of intestinal epithelial cells. *Biochem Biophys Res Commun* 2017; **485**: 468-475.

- 38 Zhang H, Guo M, Chen JH, *et al*. Osteopontin knockdown inhibits αv,β3 integrin-induced cell migration and invasion and promotes apoptosis of breast cancer cells by inducing autophagy and inactivating the PI3K/Akt/mTOR pathway. *Cell Physiol Biochem* 2014; **33**: 991-1002.
- 39 Huang RH, Quan YJ, Chen JH, *et al.* Osteopontin promotes cell migration and invasion, and inhibits apoptosis and autophagy in colorectal cancer by activating the p38 MAPK signaling pathway. *Cell Physiol Biochem* 2017; **41**: 1851-1864.
- 40 Gao X, Zhao G, Li C, *et al*. LOX-1 and TLR4 affect each other and regulate the generation of ROS in A. fumigatus keratitis. *Int Immunopharmacol* 2016; **40**: 392-399.
- 41 Yin M, Soikkeli J, Jahkola T, *et al*. Osteopontin promotes the invasive growth of melanoma cells by activating integrin alphavbeta3 and down-regulating tetraspanin CD9.
- 42 Zhao X, Guo Y, Jiang C, *et al*. JNK1 negatively controls antifungal innate immunity by suppressing CD23 expression. *Nat Med* 2017; **23**: 337-346.
- 43 Li X, Guo C, Li Y, *et al*. Ketamine administered pregnant rats impair learning and memory in offspring via the CREB pathway. *Oncotarget* 2017; **8**: 32433-32449.

44 Shuda M, Velásquez C, Cheng E, *et al*. CDK1 substitutes for mTOR kinase to activate mitotic cap-dependent protein translation. *Proc Natl Acad Sci U S A* 2015; **112**: 5875-5882.

45 Driver J, Weber C, Callaci J, *et al*. Alcohol inhibits osteopontin-dependent transforming growth factor-beta1 expression in human mesenchymal stem cells. *J Biol Chem* 2015; **290**: 9959-9973.

46 Wu TG, Wilhelmus KR, Mitchell BM. Experimental keratomycosis in a mouse model. Invest Ophthalmol Vis Sci 2003; **44**: 210-216.

47 Berger EA, McClellan SA, Vistisen KS, *et al*. HIF-1α is essential for effective PMN bacterial killing, antimicrobial peptide production and apoptosis in Pseudomonas aeruginosa keratitis. *PLoS Pathog* 2013; **9**: e1003457.

48 Gao N, Kumar A, Yu FS. Matrix Metalloproteinase-13 as a target for suppressing corneal ulceration caused by *Pseudomonas aeruginosa* infection. *J Infect Dis* 2015; **212**: 116-127.

49 Chen H, Thorne SH. Practical methods for molecular *in vivo* optical imaging. *Curr Protoc Cytom* 2012; **59**: 1–11.

50 Gutowski MB, Wilson L, Van Gelder RN, *et al. In vivo* bioluminescence imaging for longitudinal monitoring of inflammation in animal models of uveitis. *Invest Ophthalmol Vis Sci* 2017; **58**: 1521-1528.

Figure 1. Osteopontin (OPN) is increased in human A. fumigatus keratitis and A.

fumigatus-stimulated neutrophils, THP-1 macrophages, and human corneal epithelial cells (HCECs). Corneas (n = 6) from *A. fumigatus* patients and healthy donors were subjected to quantitative polymerase chain reaction (qRT-PCR) analysis for OPN (a). Then, 5- μ m paraffin sections were immunostained to visualize OPN (red) protein expression in corneas from *A. fumigatus* patients and healthy donors (b). Magnification ×200. Human neutrophils, THP-1 macrophages, and HCECs were treated with *A. fumigatus* conidia at a multiplicity of infection (MOI) of 1 at 0, 1, 4 and 16 hours for RT-PCR (c, e and g) and 0, 1/4, 1/2, 1, 4 and 16 hours for western blotting (d, f, h). The mean values and standard deviations of two independent experiments are shown. ***P*< 0.01, ****P*< 0.001

Figure 2. OPN levels are increased in *A. fumigatus* keratitis mice. Representative corneal photographs of mice *A. fumigatus* keratitis models developed by intra-stromal injection $(1 \times 10^5 \text{ conidia/cornea})$ at 0, 1/2, 1, 2, 3, 5, 7, 10 and 14 days post-infection (**a**). Corneas of six mice euthanized at corresponding times were excised and subjected to RT-PCR (**b**) and western blotting (**c**) analysis for OPN. Then, 7-µm frozen sections were immunostained to visualize OPN (red) protein expression in controls and *A. fumigatus*-infected mouse corneas in 1 day post-infection (**d**). Magnification ×400. The mean values and standard deviations of two independent experiments are shown. ***P*< 0.01, ****P*< 0.001

Figure 3. OPN production upon A. fumigatus infection is dependent on Lectin-Type Oxidized LDL Receptor 1 (LOX-1) and Erk1/2. Representative corneal photographs of mice A. fumigatus keratitis models at 1 day post-infection pretreated with siRNALOX-1 or scrambled siRNA (a). LOX-1 knockdown led to lower clinical scores (b) and higher fungal load (c). The corneas of mice (6/group) euthanized at 1 day post-infection were excised and subjected to RT-PCR (d) and western blotting (e) analysis for OPN. Effective silencing of LOX-1 was confirmed by measuring protein levels. HCECs were stimulated with A. fumigatus conidia (MOI = 1) for 16 hours after a 2-hour LOX-1 neutralization pretreatment. Cells were subjected to RT-PCR (f) and western blotting (g) analysis for OPN. Effective neutralization of LOX-1 was confirmed by decreased IL-1 β protein levels. Erk1/2 inhibitor (SCH772984) was used for pretreatment in vivo and in vitro. Mouse corneas and HCECs were subjected to RT-PCR (h and j) and western blotting (i and k) analysis for OPN after corresponding Erk1/2 inhibitor pretreatment and A. fumigatus infection. The efficacy of inhibitor in vivo and in vitro was confirmed by measuring phosphorylated Erk1/2. The mean values and standard deviations of two independent experiments are shown. *P < 0.05, ***P< 0.001 Figure 4. Disease response after siRNA_{OPN} treatment. Representative corneal photographs of mouse A. fumigatus keratitis models at 1 day (a) and 2 days (f) post-infection pretreated with siRNA_{OPN} or scrambled siRNA. OPN knockdown led to lower clinical scores at 1 day (b)

and 2 days (**g**) and higher fungal load at 1 day (**c**) and 2 days (**h**) post-infection. Effective silencing of OPN was confirmed by measuring mRNA levels at 1 day (**d**) and 2 days (**i**) and

protein levels at 1 day (e) and 2 days (j) post-infection. The mean values and standard

deviations of two independent experiments are shown. *P< 0.05, **P < 0.01, ***P< 0.001

Figure 5. siRNA_{OPN} treatment reduces neutrophil infiltration and myeloperoxidase (MPO) activity in *A. fumigatus* keratitis mice. Seven μ L frozen sections were immunostained to visualize neutrophil infiltration (green) in *A. fumigatus*-infected mouse corneas pretreated with siRNA_{OPN} or scrambled siRNA (a). Magnification ×400. Average bioluminescence from inflammation probe dropped into the surface of *A. fumigatus*-infected mouse corneas indicated that corneas of siRNA_{OPN}-pretreated mice exhibited a significant decrease in MPO levels at 1 day post-infection compared to scrambled controls by photographs (b) and photon detection (c). Corneas of mice (6/group) euthanized at 1 day post-infection were excised and subjected to a colorimetric activity assay for MPO (d). The mean values and standard deviations of two independent experiments are shown. ***P*< 0.01, ****P* < 0.001.

Figure 6. OPN-mediated IL-1β secretion in response to *A. fumigatus* infection is dependent on Eukaryotic translation initiation factor 4E-binding protein 1 (4E-BP1). Corneas of six *A. fumigatus* keratitis mice euthanized at 0, 1/2, 1, 2, 3, 5, 7, 10 and 14 days post-infection were excised and subjected to western blotting analysis for IL-1β (a). *A. fumigatus* keratitis mice (6/group) pretreated with siRNA_{OPN} or scrambled siRNA were euthanized at 1 day post-infection, and their corneas were excised and subjected to RT-PCR (b) and western blotting (c) analysis. siRNA_{OPN}-pretreated mice (6/group) were treated with or without rmOPN before *A. fumigatus* infection and euthanized 1-day post-infection. Corneas were excised and subjected to RT-PCR (d) and western blotting (e) analysis for IL-1β. An OPN neutralization antibody or IgG control was used to pretreat HCECs before *A. fumigatus* infection. HCECs were subjected to RT-PCR (f) and western blotting (g) analysis for IL-1β.

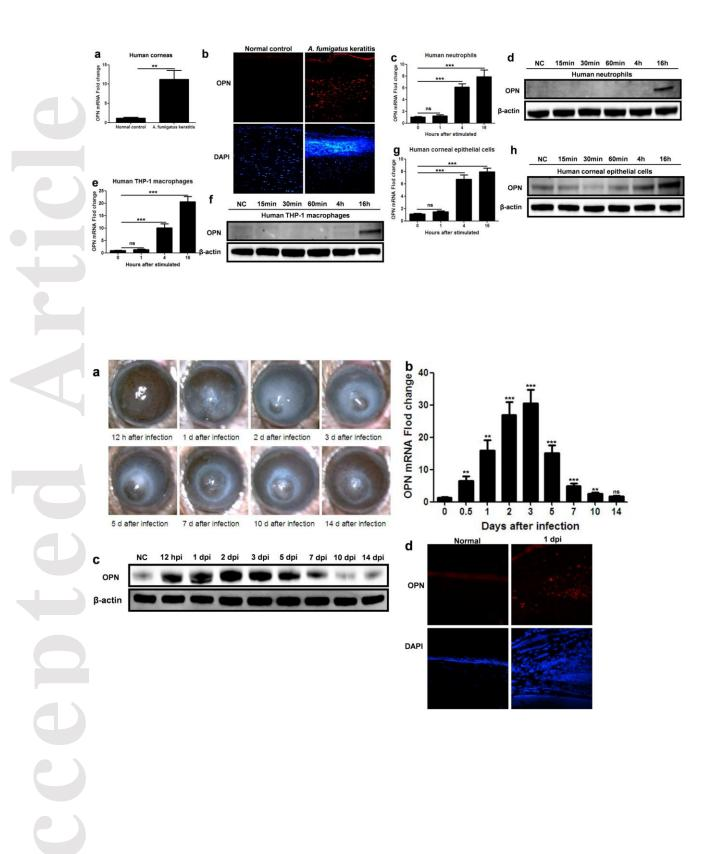
RmOPN was used for OPN neutralization antibody pretreated HCECs before *A. fumigatus* infection, and cells were subjected to RT-PCR (**h**) and western blotting (**i**) analysis for IL-1 β . A 4E-BP1/eIF4E interaction inhibitor (4E1RCat) was used to treat siRNA_{OPN}-pretreated mice and HCECs were pretreated with OPN neutralization antibody before *A. fumigatus* infection. Mouse corneas and HCECs were subjected to RT-PCR (**j** and **l**) and western blotting (**k** and **m**) analysis for IL-1 β . The mean values and standard deviations of two independent experiments are shown. **P* < 0.05, ***P*< 0.01, ****P*< 0.001

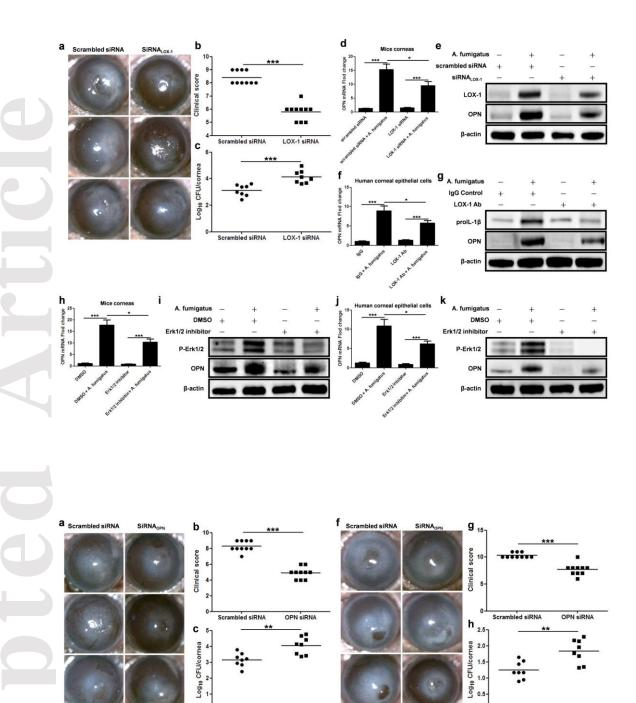
Figure 7. siRNA_{OPN} **treatment increases apoptosis in** *A. fumigatus* **keratitis mice.** Corneas of *A. fumigatus* keratitis mice (6/group) pretreated with siRNA_{OPN} or scrambled siRNA euthanized at 1 day post-infection were excised and subjected to RT-PCR analysis for Bcl-2 (a), BAX (b) and caspase-3 (c) and western blotting analysis for phosphorylated Akt, Akt, Bcl-2, BAX, cleaved-caspase-3, cleaved-caspase-9 and cleaved-caspase-8 (d). The mean values and standard deviations of two independent experiments are shown. **P*< 0.05, ***P*< 0.01, ****P*< 0.001

Supplementary figure 1. OPN production upon *A. fumigatus* infection was independent of dendritic cell-associated C-type Lectin-1 (Dectin-1) and JNK. Representative corneal photographs of *A. fumigatus* keratitis mouse models at 1 day post-infection pretreated with siRNADectin-1 or scrambled siRNA **(a).** Dectin-1 knockdown led to lower clinical scores **(b)** and higher fungal load **(c).** Corneas of mice (6/group) euthanized at 1 day post-infection

were excised and subjected to RT-PCR (**d**) and western blotting (**e**) analysis for OPN. Effective silencing of Dectin-1 was confirmed at the protein level. HCECs were stimulated with *A. fumigatus* conidia (MOI=1) for 16 hours after a Dectin-1 neutralization pretreatment for 2 hours. Cells were subjected to RT-PCR (**f**) and western blotting (**g**) analysis for OPN. Effective neutralization of Dectin-1 was confirmed by decreased IL-1 β protein levels. A JNK inhibitor (SP600125) was used for pretreatment *in vivo* and *in vitro*. Mouse corneas and HCECs were subjected to RT-PCR (**h** and **j**) and western blotting (**i** and **k**) analysis for OPN after corresponding JNK inhibitor pretreatment and *A. fumigatus* infection. Efficacy of inhibitor was confirmed *in vivo* and *in vitro* by measuring phosphorylated JNK. The mean values and standard deviations of two independent experiments are shown. ***P*< 0.01, ****P*< 0.001

Supplementary figure 2. Average bioluminescence from inflammation probe dropped into the surface of mouse cornea increased corneal MPO level after 1 day post-infection of *A*. *fumigatus* (left) compared to control (right).





0.0

A. fumigatus

scrambled siRNA

OPN

β-actin

SIRNA

j

Scrambled siRNA

OPN siRNA

0

A. fumigatus

mbled siRNA

OPN β-actin

SIRNA

е

Ort struk

d

Scrambled siRNA

OPN siRNA

i

OPN MRNA F

Mice co

On ster

